

Scale Estimation with Dual Quadrics for Monocular Object SLAM

Shuangfu Song^{†,2}, Junqiao Zhao^{*,1}, Tiantian Feng², Chen Ye¹, Lu Xiong³

Abstract—The scale ambiguity problem is inherently unsolvable to monocular SLAM without the metric baseline between moving cameras. In this paper, we present a novel scale estimation approach based on an object-level SLAM system. To obtain the absolute scale of the reconstructed map, we derive a nonlinear optimization method to make the scaled dimensions of objects conforming to the distribution of their sizes in the physical world, without relying on any prior information of gravity direction. We adopt the dual quadric to represent objects for its ability to fit objects compactly and accurately. In the proposed monocular object-level SLAM system, dual quadrics are fastly initialized based on constraints of 2-D detections and fitted oriented bounding box and are further optimized to provide reliable dimensions for scale estimation. Experiments on TUM datasets show that our approach performs better in accuracy and robustness than existing methods.

I. INTRODUCTION

Recently, object-level SLAM has achieved significant progress because of the breakthrough of convolutional neural networks (CNNs). A series of monocular object SLAM systems [1], [2], [3] are proposed. These semantically enriched SLAM algorithms can improve robot intelligence for scene understanding and human-robot interaction. However, due to the limitation of monocular sensors, the scale factor between the reconstructed map and the physical world is unknown, which is crucial for real-world applications.

The absolute scale is unobservable for a monocular camera but can be inferred with prior knowledge [4]. Previous studies [5], [6] attempted to use the Bayesian framework to infer the scale factor by associating estimated heights of observed objects with their priors. But, there are some limitations: First, when measuring the height of an object, it has to resort to the direction of gravity as the reference. Second, only specific objects with salient height can be used in the algorithm, other low objects such as “keyboard”, “book”, etc., are discarded. Objects that not standing upright are also treated as anomalous. However, these cases are common in real scenes. As a result, the accuracy and applicability of these methods are limited.

^{*}This work is supported by the National Key Research and Development Program of China (No. 2018YFB0105103, No. 2018YFB0505400), the National Natural Science Foundation of China (No. U1764261, No. 41801335, No. 41871370)

²Shuangfu Song and Tiantian Feng are with the School of Surveying and Geo-Informatics, Tongji University, Shanghai 200092, China (e-mail: 1911204@tongji.edu.cn; fengtiantian@tongji.edu.cn).

¹Junqiao Zhao and Chen Ye are with the Department of Computer Science and Technology, School of Electronics and Information Engineering, Tongji University, Shanghai 201804, China (e-mail: zhaojunqiao@tongji.edu.cn; yechen@tongji.edu.cn).

³Lu Xiong is with the Institute of Intelligent Vehicle, Tongji University, Shanghai, 201804 China (e-mail: xiong.lu@tongji.edu.cn).

In this paper, we propose a scale estimation approach by exploring all reliable dimensions of general objects without resorting to the prior gravity direction. More observations can reduce the uncertainty of scale estimation and make the scaled dimensions of objects closer to those of the real world. Hence, it is crucial to obtain accurate dimension estimation of objects for scale inferencing. To do so, we develop a monocular object SLAM system using dual quadrics as three-dimensional (3-D) object landmarks. A dual quadric can flexibly fit various 3-D shapes tightly and quadrics in dual vector space, which is well defined in projective geometry [7]. We adopt a two-stage quadric initialization strategy based on our previous work [8]. Then accurate dimensions can be extracted from quadrics reconstructed by semantic mapping. The Metric-tree, a hierarchical representation of sizes of more than 900 object categories [9], is used to provide object size priors with uncertainties. This ensures that our algorithm can cope with generic scenarios. At last, we derive a nonlinear optimization method to estimate the optimal scale factor. To the best of our knowledge, this is the first work that takes advantage of dual quadrics to estimate the scale factor within a monocular object SLAM system.

In summary, our contributions are as follows.

- 1 An accurate and robust scale estimation approach exploiting quadrics and object size priors.
- 2 A monocular object SLAM system with a semantic mapping module, which can build object-oriented maps accurately and timely.

II. RELATED WORK

A. Scale Estimation

To overcome the monocular scale ambiguity problem, an intuitive way is to leverage extra sensors, such as inertial measurement units (IMUs) [10], LiDAR [11]. Without augmented sensors, at least one absolute reference needs to be integrated. From this perspective, reference information used in existing approaches can be divided into three categories: camera setup parameters, learned models, and prior information of semantic objects.

On ground vehicle platforms, cameras are usually mounted on the vehicle firmly, which makes it possible to take the height of cameras from the ground plane as the reference. [12], [13], [14] proposed to estimate unscaled camera height by extracting the ground plane parameters from map points. Then, with the known camera height relative to the ground plane, the absolute scale can be obtained. These approaches are accurate and effective, but cannot cover more general scenarios, for example, where only unanchored hand-held cameras are available.

In [15], a monocular SLAM system was proposed to recover the scale by incorporating a depth prediction module based on deep convolutional neural fields. A similar idea is proposed in DVSO [16], in which deep depth predictions are used as virtual stereo measurements. The difference is that [16] trained the network with sparse depth reconstructions from Stereo DSO [17], instead of using depth measurements captured by a LiDAR. Another learning-based method [18] trained a space-coarse, but depth-accurate CNN for depth prediction, and directly estimated the scale factor for every frame. These approaches have achieved impressive performance on KITTI datasets. However, it is still a challenge for them to generalize to different environments.

To exploit the semantic objects priors, methods in [5] and [6] adopt the Bayesian framework incorporating the height priors of objects to infer the global scale. Recent work [9] improved this approach by introducing not only heights but all available dimensions of objects into the scale estimation. These approaches require the gravity direction known and objects to be placed upright to measure the size of objects.

B. Object SLAM

Classic visual SLAM systems have been well explored in the representation of geometric primitives like points, lines, and planes. SLAM++ [19] is considered as the first object-level SLAM system which used an RGB-D camera to detect objects by matching prior CAD models. Similarly, a real-time monocular object SLAM proposed in [20] leveraged a large object database and uses bags of words to recognize objects. Later, more general object models were adopted in the following studies in order to break the limitations of the pre-prepared object database. [21] represented objects as spheres to incorporate them into bundle adjustment as extended points. QuadricSLAM [1] was proposed to use dual quadric to represent objects flexibly. CubeSLAM [2] described objects using cuboids. Inspired by them, EAO-SLAM [3] adopted both quadrics and cuboids to represent objects based on their prior shape. Recently, superquadrics was also introduced into object-oriented semantic SLAM [22], which is a meaningful exploration.

III. SCALE FACTOR ESTIMATION

A. Problem Formulation

We describe a general 3-D object using quadrics with nine parameters: 6 DoF pose and three dimensions i.e. length, width and height. We denote d as a unscaled dimension of reconstructed objects, \tilde{d} as its real length. The scale factor s can be expressed as

$$s = \frac{\tilde{d}}{d}. \quad (1)$$

Then the reconstructed map can be corrected by this scale. However, each dimension can calculate a different local scale factor through its prior length. This requires us to use all dimensions as conditions to find a global optimal scale. Therefore, we assume that dimensions are conforming to Gaussian distributions $N(\mu, \sigma)$, and are independent of each

other. With the set of all dimensions $D = \{d_i\}$ of objects, the conditional probability of scale s is presented as

$$P(s|D) \propto \prod_i P(d_i|s) \quad (2)$$

Our goal is to find the scale which maximizes the probability according to the distribution of dimensions. The likelihood can be presented as

$$P(d_i|s) = N(\mu_i, \sigma_i) \quad (3)$$

where μ_i and σ_i are prior parameters to describe the distribution of d_i . The error between d_i and its expectation is defined as

$$e_i = \mu_i - sd_i. \quad (4)$$

The maximum likelihood estimation (MLE) can be formulated as a least-squares optimization problem

$$s^* = \arg \min_s \sum_i \left\| \frac{e_i}{\sigma_i} \right\|^2 \quad (5)$$

B. Object Uncertainty Model

As shown in Equation 5, the uncertainty of a dimension is modeled by its variance calculated by size statistics from Metric-tree [9]. This is not sufficient because the accuracy of scale estimation is also affected by the quality of the object reconstruction. A dual quadric is reconstructed from observations of multi-view 2-D detections and 3-D map points, which will be explained detailedly in Section IV. We define a confidence c based on these observations to evaluate the reliability of a dual quadric:

$$c = \frac{w_1 c_{det} + w_2 c_{pt} + w_3 c_{vis}}{w_1 + w_2 + w_3} \quad (6)$$

where w_1, w_2, w_3 are weight parameters.

c_{det} is the confidence of 2-D detection and is derived by:

$$c_{det} = \frac{1}{n} \sum_k p_k$$

where p_k is the probability of detection obtained from the 2-D object detector in view k .

c_{pt} is the confidence of map points and is derived by:

$$c_{pt} = \min(1, \max(0, \log_a N_p))$$

where N_p is the total number of map points associated with the object.

c_{vis} is the confidence of visibility and is derived by:

$$c_{vis} = \min(1, \max(0, \log_b N_o))$$

where N_o is the total number of 2D detections. a, b are super parameters.

Lastly, Equation 5 can be reformulated by integrating the confidence weight as

$$s^* = \arg \min_s \sum_i \left\| \frac{c_i e_i}{\sigma_i} \right\|^2. \quad (7)$$

C. Object Dimensions Selection

Besides the object uncertainty, the reliability of the dimensions of an object should also be taken into account. For example, dimensions like the height of “bottle”, length of “spoon” are more stable than the thickness of “book” and “keyboard”. This is because relatively small dimensions are difficult to estimate accurately during the mapping process. Therefore, objects are classified into three categories according to their dimensions. We denote three dimensions of an object as d_1, d_2, d_3 following $d_1 \geq d_2 \geq d_3 > 0$. Then the shape feature of an object can be defined as:

$$L_d = \frac{d_1 - d_2}{d_1} \quad P_d = \frac{d_2 - d_3}{d_1} \quad S_d = \frac{d_3}{d_1} \quad (8)$$

where L_d , P_d , S_d are linearity, planarity, and scattering, respectively [23]. For an object with $S_d < 0.3$, it belongs to the pole-like when $L_d > 0.5$; and belongs to the disk-like object when $P_d > 0.5$. Otherwise it belongs to others. For a pole-like object, only the longest dimension of it is stable enough to be used. For a disk-like object, the shortest dimension of it should be discarded. For others, all dimensions can provide useful hints for scale inferencing.

D. Outliers Elimination

False 2-D object detections lead to the erroneous association between 3D objects and their corresponding size priors, thereby reducing the accuracy of scale estimation. We found that local scale factors estimated by most dimensions are relatively close to each other, which is consistency. Based on this, outliers caused by false detection can be detected and eliminated by statistical methods such as the boxplot. First, all local scales are sorted in ascending order. Then the interquartile range (IQR) is defined as $IQR = Q_3 - Q_1$, where Q_1 is the first quartile and Q_3 is the third quartile. A dimension will be discarded if its local scale factor is less than $Q_1 - 1.5IQR$ or greater than $Q_3 + 1.5IQR$.

E. Implementation

Our scale estimation pipeline is shown in Figure 1. We first select all stable dimensions from map objects and calculate their local scales with prior dimension distribution for outliers elimination. Then we combine the prior variance of the dimension and the confidence of the reconstructed object to weight each error term of the scale optimization process. Scale estimation is embedded in the back-end optimization process of our SLAM system as described in Section IV. Every time the object map is updated, a new scale factor will be calculated automatically by g2o [24], and then be used to scale the whole map.

IV. SEMANTIC MAPPING

A. Overview

To acquire accurate object size for scale estimation, we build an object SLAM system based on ORB-SLAM2 [25]. Only keyframes created by camera tracking are used for object detection. Then dual quadrics are initialized from 2-D bounding boxes and 3-D points in the semantic mapping

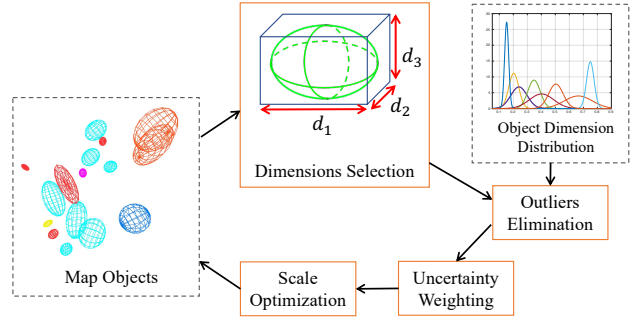


Fig. 1. The pipeline of scale estimation.

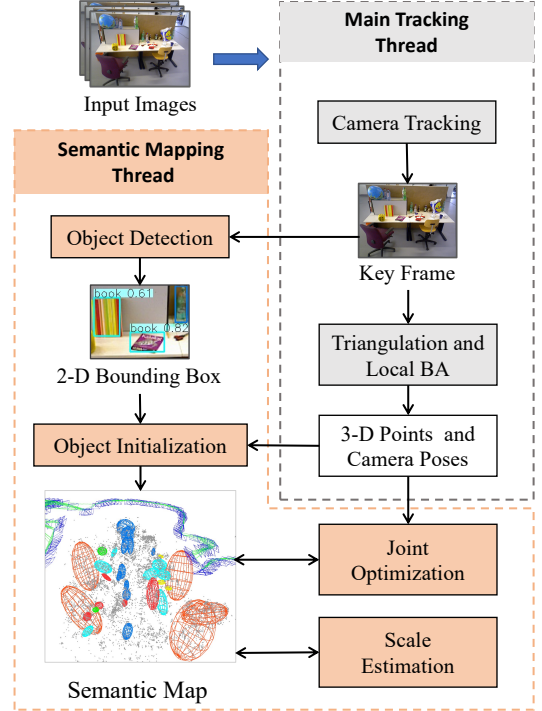


Fig. 2. The proposed object SLAM system framework.

thread. At last, all objects, points and camera poses are jointly optimized to update the semantic map. The framework of the system is shown in Figure 2.

B. Dual Quadric Initialization

A 3-D dual quadric can be initialized from a set of planar constraints constructed by multi-view detections for this object, as done in [1]. However, this method only works when enough detections with diverse viewpoints are accumulated. Our previous work [8] constructed a 3-D convex hull from map points to provide valid planar constraints for dual quadric initialization. However, building the 3-D convex-hull is time-consuming. In this paper, we propose an efficient two-stage approach for dual quadric initialization.

We first associate 3-D map points to their corresponding object if points are projected into the 2-D bounding box of this object. Then the 3-D oriented bounding box (OBB) is extracted from associated map points to directly provide initial parameters (orientation, position, size) for dual quadrics.

Here, the adopted covariance-based OBB fitting algorithm is proposed in [26]. With the accumulation of measurements, the dual quadric will be re-initialized from 2-D detections if the new one is more accurate. In this way, the dual quadrics can be initialized successfully at different stages to avoid the problem of latency.

C. Joint Optimization

After initialization, objects are further optimized jointly with other map components. Denote the set of camera poses, quadric object and points as $X = \{x_i \in SE(3)\}$, $Q = \{q_j \in \mathbb{R}^{4 \times 4}\}$ and $P = \{p_k \in \mathbb{R}^3\}$, respectively. Three types of measurement errors are introduced into the bundle adjustment.

1) *Camera-Object Measurement Error*: A dual quadric, represented by a 4×4 symmetric matrix Q^* , can be projected onto an image plane to obtain a dual conic represented by 3×3 symmetric matrix C^* , following this rule:

$$C^* = H Q^* H^T \quad (9)$$

where $H = K[R|t]$ is the camera projection matrix composed of camera intrinsic and extrinsic parameters. As done in [27], we can obtain the predicted 2-D bounding box $\hat{\mathbf{b}} = [\hat{u}_{max}, \hat{v}_{max}, \hat{u}_{min}, \hat{v}_{min}]$ of the dual quadric by

$$\hat{u}_{max}, \hat{u}_{min} = \frac{1}{C_{3,3}^*} (C_{1,3}^* \pm \sqrt{C_{1,3}^{*2} - C_{1,1}^* C_{3,3}^*}) \quad (10)$$

$$\hat{v}_{max}, \hat{v}_{min} = \frac{1}{C_{3,3}^*} (C_{2,3}^* \pm \sqrt{C_{2,3}^{*2} - C_{2,2}^* C_{3,3}^*}) \quad (11)$$

where $[u_{max}, v_{max}], [u_{min}, v_{min}]$ represent the top left and bottom right corners of the 2-D box, respectively. Denote the 2-D bounding box measurement observed by object detector as \mathbf{b} . Given a camera pose x , and a 3-D object q , the 4-D re-projected error can be defined as

$$\mathbf{e}(x, q) = \hat{\mathbf{b}} - \mathbf{b} \quad (12)$$

2) *Camera-Point Measurement Error*: The standard 3-D point reprojection error is preserved as the backbone of optimization process:

$$\mathbf{e}(x, p) = \pi(T_c^{-1}p) - z \quad (13)$$

where $\pi(\cdot)$ is the camera projective function, T_c is the camera pose, and z is the pixel coordinate measurement.

3) *Object-Point Measurement Error*: To exploit constraints between map objects and map points, we introduce a novel measurement error:

$$\mathbf{e}(q, p) = \max(0, \sqrt{p^T Q p} + 1 - 1) \quad (14)$$

where Q is the primal quadric matrix with $Q_{4,4} = -1$. As shown in Figure 3, when point p is outside the ellipsoid, p^* is the intersection point between the line segment \overline{op} and the quadric surface. the error represent the ratio $\overline{op^*}/\overline{p^*p}$. We use the max operator to encourage the quadric to wrap the associated map points. When a point lies inside the quadric, its measurement error will be zero.

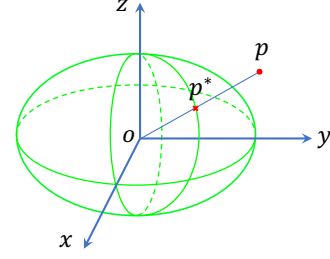


Fig. 3. The measurement error between quadrics and points.

Lastly, combining all measurement error items, the optimization problem can be formulated as

$$X^*, Q^*, P^* = \arg \min_{\{X, Q, P\}} \left\{ \sum_{i,j} \|e(x_i, q_j)\|_{\Omega_{ij}}^2 + \sum_{i,k} \|e(x_i, p_k)\|_{\Omega_{ik}}^2 + \sum_{j,k} \|e(q_j, p_k)\|_{\Omega_{jk}}^2 \right\} \quad (15)$$

where Ω is the covariance matrix of different error measurements for Mahalanobis norm. This nonlinear least-squares problem can be solved efficiently using Levenberg-Marquardt algorithm.

V. EXPERIMENTS

We evaluate the performance of our scale estimation approach on TUM RGB-D datasets. For monocular object SLAM, only RGB images are input and YOLOv3 [28] are adopted for 2-D object detection. We adopt the relative scale error (RSE) as the evaluation metric of scale estimation:

$$\text{RSE} = \frac{|\hat{s} - s|}{s} \quad (16)$$

where \hat{s} is our estimated global scale factor of the scene, and s is the ground truth scale factor which can be obtained from the similarity transformation $S = \{s, R, t\}$ between the trajectory estimated by our SLAM algorithm and the ground truth trajectory as following:

$$S^* = \arg \min_{\{s, R, t\}} \sum_i \|p_i - sR\hat{p}_i - t\|^2 \quad (17)$$

where \hat{p}_i, p_i represent the position of estimated trajectory, groundtruth trajectory respectively.

A. Scale Estimation Results

There are two works [5], [9] similar to ours. The latter uses an structure-from-motion (SfM) system running offline to reconstruct 3-D scenes and uses a pixel-wise instance segmentation method to extract objects from the reconstructed point cloud, which is difficult to compare with our method fairly. Therefore, the former is chosen as our baseline. The identical object size priors and the outliers rejection algorithm based on scale consistency are used in both methods.

We select three sequences with common objects from TUM datasets for evaluation and run each algorithm 10 times on all sequences to calculate the average RSE and its standard deviation. As shown in Table I, our method achieves

TABLE I
COMPARISON OF SCALE ESTIMATION ON TUM DATASET

seq	Sucar's [5]		ours	
	RSE(%)	std	RSE(%)	std
fr1-desk	13.89	5.78	4.35	3.51
fr2-desk	5.50	2.58	3.63	1.22
fr3-office	9.49	3.02	6.27	2.60

RSE of around 5% which outperforms the baseline in a big margin.

In the fr1-desk sequence, the baseline method performed not well because there are few objects with stable height can be used as reference in this scene, which is shown in the left image of Figure 4(c). Our method effectively utilizes the size information of “book” and “keyboard” in this scene, and obtains more accurate and robust results. In the remaining two sequences, although there are more object height clues available for the baseline method, our method still performs better. This is because the object height measuring of the baseline is limited by 2-D detection results, thereby is easily affected by object occlusion. Meanwhile, our method exploits multi-view observations of the object to reduce the uncertainty of dimension measurement, which improves the performance of scale estimation. In addition, it can be noticed that the performance of scale estimation in the fr3-office sequence is not as good as in other scenes, even though there are the most objects available in this scene. The main reason is that many bottles in this scene exceed the regular size in Metric-tree and the dimensions of these bottles have relatively large contribution in scale estimation.

B. Qualitative Results

The qualitative evaluation results of scale estimation and semantic mapping are shown in Figure 4. Figure 4(a) shows the comparison between the ground truth and the scale-recovered trajectory estimated by our system without further scale alignment. EVO [29] is used to visualize the trajectories. Figure 4(b) shows that the object-oriented maps built by our system can express the environment well and are understandable with semantic information. Figure 4(c) shows the projection of all dual quadrics onto the images. It can be seen that the reconstructed quadrics can fit objects in the scene accurately.

C. Ablation Study

For the base scheme of scale estimation, only the most prominent dimensions of objects are input into the scale optimization with its corresponding prior variance as weights. As explained in Section III, three other schemes are designed to enhance our method: outliers elimination, dimensions selection and uncertainty model. We conduct an ablation study to evaluate their effects on scale estimation. The results are shown in Table II. It can be seen that the relative scale errors are significantly diminished after the process of outliers rejection based on scale consistency. This is because we get rid of the objects with wrong semantic labels from the false 2-D object detections. Then, by introducing more

TABLE II
ABLATION STUDY OF DIFFERENT OPTIONAL SELECTING RESULTS

out ¹	dim ²	uncer ³	fr1-desk		fr2-desk		fr3-office	
			RSE(%)	std	RSE(%)	std	RSE(%)	std
			10.81	6.56	9.10	3.40	14.51	4.59
✓			4.84	3.37	5.98	1.94	7.88	3.70
✓	✓		4.48	3.37	3.79	1.28	6.44	2.91
✓	✓	✓	4.35	3.51	3.63	1.22	6.27	2.60

¹ Outliers elimination. ² Dimensions selection. ³ Uncertainty model.

reliable dimensions in the scale optimization, the accuracy and robustness of our method are improved. Lastly, we adopt the uncertainty model to assign appropriate weights to each error term, and the best performance is achieved.

VI. CONCLUSION

In this paper, we present an accurate and robust scale estimation approach that takes the object size priors as the absolute reference. We develop a monocular object SLAM system to reconstruct objects as dual quadrics to provide reliable dimensions for scale estimation with no resort to assumptions on the gravity direction. In return, the estimated scale factor can be used to recover the absolute scale of the whole map built by our SLAM system. Quantitative and qualitative experiments demonstrate the outstanding performance of our method. In the future, we intend to extend our algorithm to cope with the large-scale outdoor environment, in which the scale drift problem should be emphatically considered. Moreover, methods of collecting and modeling prior object size information are also worth exploring.

REFERENCES

- [1] L. Nicholson, M. Milford, and N. Sünderhauf, “QuadricSLAM: Dual Quadrics From Object Detections as Landmarks in Object-Oriented SLAM,” *IEEE Robotics and Automation Letters*, vol. 4, no. 1, pp. 1–8, 2019.
- [2] S. Yang and S. Scherer, “CubeSLAM: Monocular 3-D Object SLAM,” *IEEE Transactions on Robotics*, vol. 35, no. 4, pp. 925–938, 2019.
- [3] Y. Wu, Y. Zhang, D. Zhu, Y. Feng, S. Coleman, and D. Kerr, “EAO-SLAM: Monocular Semi-Dense Object SLAM Based on Ensemble Data Association,” in *2020 IEEE/RSJ International Conference on Intelligent Robots and Systems (IROS)*. IEEE, 2020, pp. 4966–4973.
- [4] T. Konkle and A. Oliva, “A Real-World Size Organization of Object Responses in Occipitotemporal Cortex,” *Neuron*, vol. 74, no. 6, pp. 1114–1124, 2012.
- [5] E. Sucar and J.-B. Hayet, “Probabilistic Global Scale Estimation for MonoSLAM Based on Generic Object Detection,” in *2017 IEEE Conference on Computer Vision and Pattern Recognition Workshops (CVPRW)*. IEEE, 2017, pp. 988–996.
- [6] E. Sucar and J.-B. Hayet, “Bayesian Scale Estimation for Monocular SLAM Based on Generic Object Detection for Correcting Scale Drift,” in *2018 IEEE International Conference on Robotics and Automation (ICRA)*. IEEE, 2018, pp. 5152–5158.
- [7] R. Hartley and A. Zisserman, *Multiple View Geometry in Computer Vision*. Cambridge, U.K.: Cambridge Univ. Press, 2004.
- [8] S. Chen, S. Song, J. Zhao, T. Feng, C. Ye, L. Xiong, and D. Li, “Robust Dual Quadric Initialization for Forward-Translating Camera Movements,” *IEEE Robotics and Automation Letters*, vol. 6, no. 3, pp. 4712–4719, 2021.
- [9] S. Zhang, X. Li, Y. Liu, and H. Fu, “Scale-aware Insertion of Virtual Objects in Monocular Videos,” in *2020 IEEE International Symposium on Mixed and Augmented Reality (ISMAR)*. IEEE, 2020, pp. 36–44.
- [10] G. Nützi, S. Weiss, D. Scaramuzza, and R. Siegwart, “Fusion of IMU and Vision for Absolute Scale Estimation in Monocular SLAM,” *Journal of Intelligent & Robotic Systems*, vol. 61, no. 1, pp. 287–299, 2011.

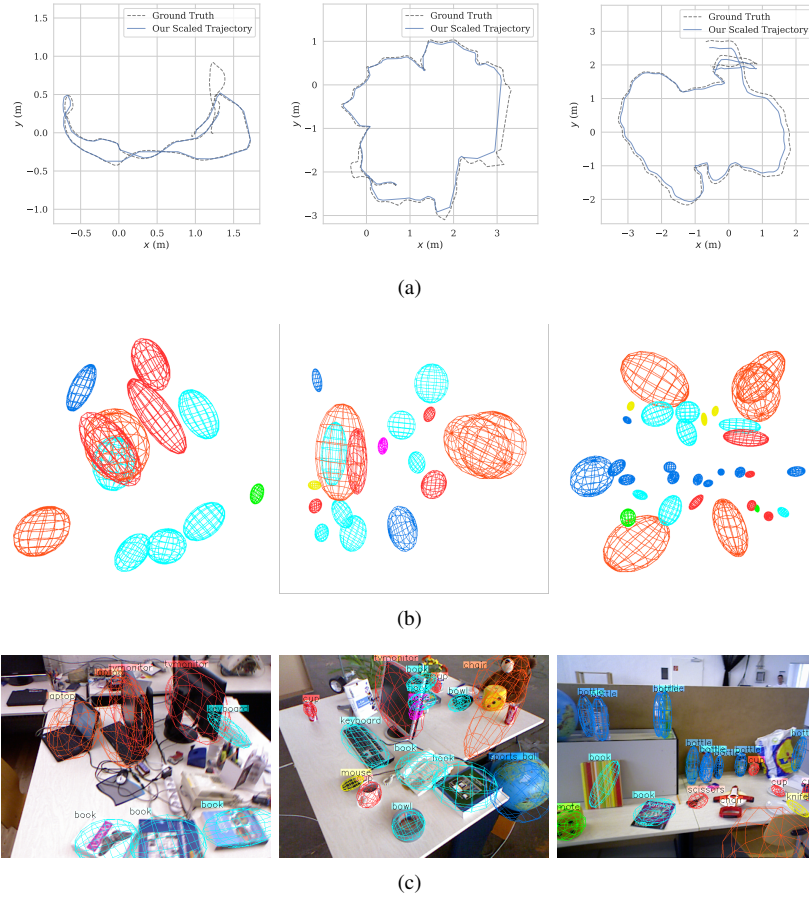


Fig. 4. The qualitative results of scale estimation and semantic mapping. The left column, middle column and right column are results on sequence fr1_desk, fr2_desk and fr3_desk, respectively. (a) Comparisons between the ground truth (gray) and our scaled trajectories (blue). (b) The object map built by our object SLAM. (c) The 2-D projection of reconstructed quadrics on the image.

- [11] Z. Zhang, R. Zhao, E. Liu, K. Yan, and Y. Ma, “Scale Estimation and Correction of the Monocular Simultaneous Localization and Mapping (SLAM) Based on Fusion of 1D Laser Range Finder and Vision Data,” *Sensors*, vol. 18, no. 6, p. 1948, 2018.
- [12] S. Song and M. Chandraker, “Robust Scale Estimation in Real-Time Monocular SFM for Autonomous Driving,” in *2014 IEEE Conference on Computer Vision and Pattern Recognition*. IEEE, June 2014, pp. 1566–1573.
- [13] Dingfu Zhou, Y. Dai, and Hongdong Li, “Reliable scale estimation and correction for monocular Visual Odometry,” in *2016 IEEE Intelligent Vehicles Symposium (IV)*. IEEE, 2016, pp. 490–495.
- [14] X. Wang, H. Zhang, X. Yin, M. Du, and Q. Chen, “Monocular Visual Odometry Scale Recovery Using Geometrical Constraint,” in *2018 IEEE International Conference on Robotics and Automation (ICRA)*. IEEE, 2018, pp. 988–995.
- [15] X. Yin, X. Wang, X. Du, and Q. Chen, “Scale Recovery for Monocular Visual Odometry Using Depth Estimated with Deep Convolutional Neural Fields,” in *2017 IEEE International Conference on Computer Vision (ICCV)*. IEEE, 2017, pp. 5871–5879.
- [16] N. Yang, R. Wang, J. Stückler, and D. Cremers, “Deep virtual stereo odometry: Leveraging deep depth prediction for monocular direct sparse odometry,” in *Proceedings of the European Conference on Computer Vision (ECCV)*. Springer International Publishing, 2018, pp. 835–852.
- [17] R. Wang, M. Schworer, and D. Cremers, “Stereo DSO: Large-Scale Direct Sparse Visual Odometry With Stereo Cameras,” in *Proceedings of the IEEE International Conference on Computer Vision*. IEEE, 2017, pp. 3903–3911.
- [18] W. N. Greene and N. Roy, “Metrically-Scaled Monocular SLAM using Learned Scale Factors,” in *2020 IEEE International Conference on Robotics and Automation (ICRA)*. IEEE, 2020, pp. 43–50.
- [19] R. F. Salas-Moreno, R. A. Newcombe, H. Strasdat, P. H. Kelly, and A. J. Davison, “SLAM++: Simultaneous Localisation and Mapping at the Level of Objects,” in *2013 IEEE Conference on Computer Vision and Pattern Recognition*. IEEE, June 2013, pp. 1352–1359.
- [20] D. Gálvez-López, M. Salas, J. D. Tardós, and J. M. M. Montiel, “Real-time monocular object SLAM,” *Robotics and Autonomous Systems*, vol. 75, pp. 435–449, 2016.
- [21] D. Frost, V. Prisacariu, and D. Murray, “Recovering Stable Scale in Monocular SLAM Using Object-Supplemented Bundle Adjustment,” *IEEE Transactions on Robotics*, vol. 34, no. 3, pp. 736–747, 2018.
- [22] F. Tschopp, J. Nieto, R. Siegwart, and C. D. Cadena Lerma, “Superquadric Object Representation for Optimization-based Semantic SLAM,” 2021.
- [23] M. Weinmann, B. Jutzi, and C. Mallet, “Semantic 3D scene interpretation: A framework combining optimal neighborhood size selection with relevant features,” *ISPRS Annals of the Photogrammetry, Remote Sensing and Spatial Information Sciences*, vol. II-3, pp. 181–188, 2014.
- [24] R. Kümmerle, G. Grisetti, H. Strasdat, K. Konolige, and W. Burgard, “G2o: A general framework for graph optimization,” in *2011 IEEE International Conference on Robotics and Automation*. IEEE, 2011, pp. 3607–3613.
- [25] R. Mur-Artal and J. D. Tardós, “ORB-SLAM2: An Open-Source SLAM System for Monocular, Stereo, and RGB-D Cameras,” *IEEE Transactions on Robotics*, vol. 33, no. 5, pp. 1255–1262, 2017.
- [26] S. A. Gottschalk, “Collision queries using oriented bounding boxes,” Ph.D., The University of North Carolina at Chapel Hill, 2000.
- [27] K. Ok, K. Liu, K. Frey, J. P. How, and N. Roy, “Robust Object-based SLAM for High-speed Autonomous Navigation,” in *2019 International Conference on Robotics and Automation (ICRA)*. IEEE, 2019, pp. 669–675.
- [28] J. Redmon and A. Farhadi, “YOLOv3: An Incremental Improvement,” *arXiv e-prints*, 2018.

- [29] M. Grupp, “evo: Python package for the evaluation of odometry and slam.” <https://github.com/MichaelGrupp/evo>, 2017.